

Wireless Implantable EMG Sensing Microsystem

Bradley D. Farnsworth, Ronald J. Triolo*, and Darrin J. Young

Department of Electrical Engineering and Computer Science, *Department of Orthopaedics and Biomedical Engineering
Case Western Reserve University, Cleveland, Ohio 44106

Email: farns@ieee.org

Abstract—This paper presents a wireless, subfascially implantable electromyogram (EMG) sensing microsystem design for intelligent myoelectric control of powered prostheses. The implantable system consists of two Pt-Ir epimysial EMG electrodes, a custom-designed ASIC, and an RF telemetry coil and is capable of wirelessly transmitting digitized EMG data to an external telemeter mounted in a prosthetic socket. The prototype microsystem is powered by a near-field inductive link operating at 8 MHz with 10% DC power transfer efficiency. On-chip rectification and regulation produce stable 2 V and 2.7 V supplies with a DC current driving capability up to 100 μ A. The EMG electrodes are interfaced with a differential capacitively-coupled amplifier with 38 dB closed-loop gain, 1 kHz bandwidth, and 78 nV/ $\sqrt{\text{Hz}}$ input-referred noise floor. The amplified EMG signal is then digitized on chip using an 11-bit algorithmic ADC. The digital EMG data can be Manchester-coded and transmitted to the external telemeter using phase shift keying (PSK) modulation scheme on the same wireless link as the inductive powering system.

I. INTRODUCTION

Myoelectric signals are critical natural control sources for enhanced biomimetic performance of powered prosthetic lower limbs [1]. Previous implementations of myoelectrically controlled prosthetic lower limbs rely on surface EMG recorded using either electrodes in the prosthetic socket or by using skin patch electrodes attached to the residual limb. The former option precludes the use of a prosthetic sock, which causes uncomfortable friction between the socket and the residual limb. The latter option requires the user to prepare the skin surface and attach the electrodes and lead wires daily. Both options are prone to motion artifacts and poor connections due to perspiration. A fully implantable EMG sensor obviates these issues by measuring muscle activity directly from the muscle surface, allowing for the use of a prosthetic sock, and eliminating any additional steps when donning the prosthesis.

Wireless inductively coupled systems have been implemented for many applications, where it is impractical or impossible to connect a sensor directly to processing or actuation systems [2-4]. This is especially true in biomedical implants where wires passing through the skin are prone to infection. In the battery-less microsystem presented here, a class-E RF power amplifier drives a series-tuned resonant spiral coil located outside the body. A miniature parallel-tuned resonant coil is positioned coaxially with respect to the transmitting coil with a separation distance of up to 2 cm, corresponding to the typical skin thickness for this application. Passive phase-shift keying

(PSK) digital data telemetry, which uses the same wireless inductive link as the powering system [4], is selected for this microsystem design due to the relatively high obtainable data rate and static coupling factor of the coils.

In this paper, an EMG sensing microsystem with wireless power and data telemetry capability for intelligent prosthesis control applications is presented. The remote powering system produces stable DC power supplies of 2 V and 2.7 V, providing 83 μ A for the integrated electronics. The implantable system can transmit a single channel of 50 kbps Manchester-coded EMG data to the external transceiver over an 8 MHz RF powering link. The demonstrated system performance is adequate for intelligent prosthesis control.

II. WIRELESS MICROSYSTEM ARCHITECTURE

The proposed EMG sensing microsystem is designed to stream real-time EMG data when the implantable coil is brought into alignment with the external power transmitting coil. Figure 1 depicts an external transceiver mounted in a prosthetic socket with a wireless link coupled to the implanted EMG sensor.

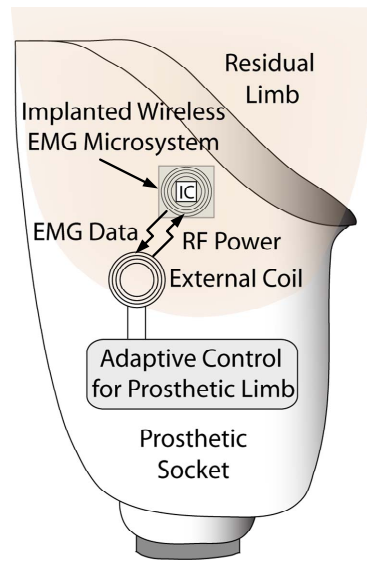


Figure 1. Prosthetic interface architecture.

Figure 2 presents the overall microsystem architecture, consisting of the wireless power and data telemetry link and integrated EMG sensing and analog-to-digital conversion (ADC) circuits.

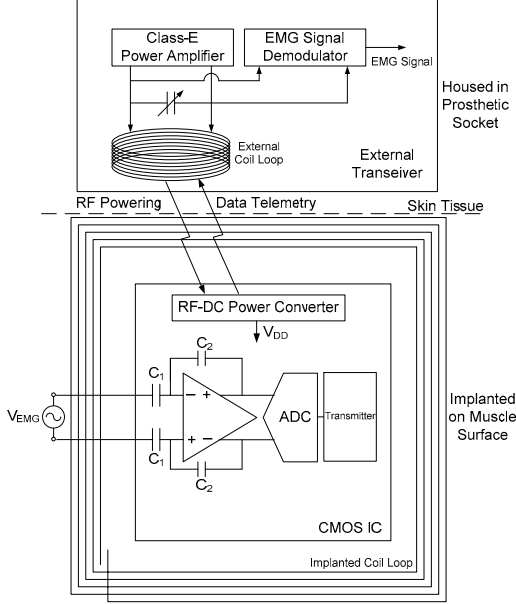


Figure 2. EMG sensing microsystem architecture.

The implantable system is powered wirelessly by inductively coupled coils. Figure 3 shows a simplified diagram of the wireless powering system.

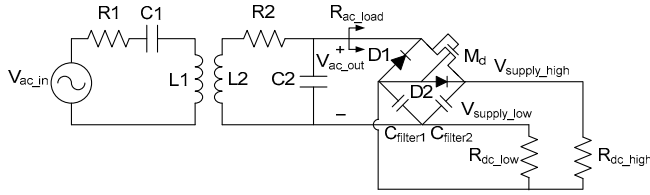


Figure 3. Simplified wireless powering architecture.

An RF input signal, V_{ac_in} , drives a set of tuned LC resonators to couple the RF energy into the implantable electronics. An on-chip voltage doubler converts the RF signal to V_{supply_high} and V_{supply_low} , which are further processed by a linear regulator to generate a stable DC voltage to power the EMG sensing microsystem. R_{dc_low} and R_{dc_high} are the modeling resistors representing the loading from the on-chip regulator. The resistive AC load, R_{ac_load} , can be expressed in terms of R_{dc_low} , R_{dc_high} , the regulated DC voltage levels, and the voltage drop across the diodes in the rectifier, as shown in Equation (1).

$$R_{ac_load} = \frac{R_{dc_low}}{2} \left(1 + \frac{V_{diode}}{V_{dc_low}} \right) \parallel \frac{R_{dc_high}}{8} \left(1 + \frac{V_{diode}}{V_{dc_high}} \right) \quad (1)$$

The voltage gain from the transmitter RF signal source to the implanted tank voltage can be defined as [2,3]

$$A_V = \frac{V_{ac_out}}{V_{ac_in}} = \frac{\omega^2 M L_2}{(\omega M)^2 + R_1 R_2 + R_1 \frac{(\omega L_2)^2}{R_{ac_load}}} \quad (2)$$

The system power transfer efficiency can be expressed as Equation (3).

$$\eta_{eff_total} = (A_V)^2 \times \left(\frac{R_1}{R_{ac_load}} \right) \times \eta_{class-E} \quad (3)$$

where $\eta_{class-E}$ is the power efficiency of a class-E amplifier with a typical value of $> 90\%$ when properly tuned. The RF operating frequency is selected for optimal biomedical operation and power transfer efficiency. An operating frequency of less than 10 MHz is desirable for $< 2\%$ RF power dissipation in the tissue between the coils [6]. A 7 μH , 6-mm-diameter implantable planar spiral coil consisting of 30 turns of 36 AWG enameled wire was built to fit around a 2 mm x 2 mm IC to reduce the overall system thickness for a compact design. A number of spiral and solenoid external coils were fabricated using 26 AWG enameled wire with 2 cm outer diameters for planar configuration and alignment in a prosthetic socket. Each coil was characterized from 1 MHz to 10 MHz using an impedance analyzer and DC power transfer efficiency was predicted using Equation (3) with $R_{ac_load} = 3.9 \text{ k}\Omega$. The coils with the best predicted gain, a 2 μH , 10-turn spiral and a 2.6 μH , 10-turn solenoid, were then tested at several frequencies to verify the accuracy of the prediction. Predicted and measured power transfer efficiency data with 1 cm coil separation are presented for these two coils with in Figure 4. The spiral coil exhibits higher coupling due to its planar geometry, enabling a shorter mean separation distance between the external and implanted coils and is selected the prototype design. An operating frequency of 8 MHz is selected for a maximum DC power transfer efficiency of 10%.

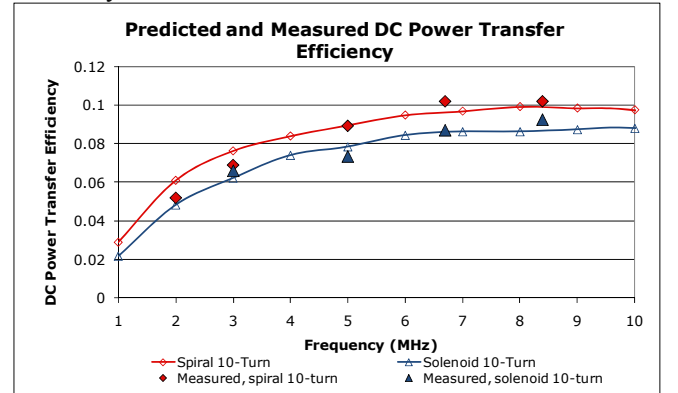


Figure 4. DC power transfer efficiency data.

Implantable epimysial Pt-Ir EMG sensing electrodes developed by the Cleveland FES Center are interfaced with an integrated CMOS low-noise, low-power differential amplifier based on a subthreshold design. EMG signals of interest for prosthetic control exhibit a bandwidth of approximately 1 kHz with a maximum energy contained within 250 Hz, and maximum signal amplitude of 10 mVpp. The minimum detectable EMG signal is typically 5 μVpp . The front-end amplifier is capacitively coupled to the sensing electrodes with a -3 dB bandwidth of 1 kHz. A fully differential architecture achieves a high common-mode

rejection ratio, critical for sensing *in vivo* real-time physiological signals.

The EMG interface amplifier is designed as a telescopic operational transconductance amplifier (OTA) with a PMOS differential input pair operating in the subthreshold or weak inversion region, as presented in Figure 5 with a 2V supply for low power dissipation.

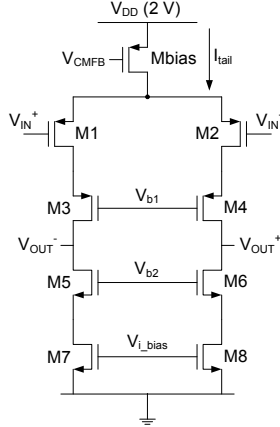


Figure 5. OTA Topology

The amplifier input-referred thermal voltage noise is dominated by the PMOS input pair, M1 and M2, and the NMOS transistors, M7 and M8, and is calculated as Equation (4).

$$\tilde{v}_{n,in,RMS} = \sqrt{2 \cdot \frac{2 \cdot 4kT}{3 \cdot g_{m1,2}} \left(1 + \frac{g_{m7,8}}{g_{m1,2}} \right)} \quad (4)$$

With a properly designed ratio of $g_{m7,8} / g_{m1,2}$, the bandwidth of 1 kHz sets the noise floor requirement at $63 \text{ nV}/\sqrt{\text{Hz}}$ with a corresponding $g_{m1,2}$ of $8.34 \text{ }\mu\text{S}$. Subthreshold design technique [5] yields a W/L ratio of approximately 8 of M1 and M2 with a bias current of $0.42 \text{ }\mu\text{A}$. Final device dimensions ($W=27.2 \text{ }\mu\text{m}$ and $L=3.2 \text{ }\mu\text{m}$) is chosen to minimize the $1/f$ noise corner below 25 Hz.

DC baseline stabilization of the OTA is achieved by using active MOS resistor elements in the feedback path in parallel with the feedback capacitor [5]. This sets a high-pass filter with a corner frequency of approximately 20 mHz, and provides a DC path from amplifier output to input. The output common-mode level of the OTA is set by a continuous time common-mode feedback circuit, which controls the voltage on the gate of MBias to set the common-mode level at 0.7 V.

The output of the EMG front-end amplifier is sampled by a switched-capacitor $2.5\times$ differential gain stage, which consumes $3 \text{ }\mu\text{A}$ from 2 V supply, as shown in Figure 6. The $2.5\times$ gain stage drives a fully differential 11-bit algorithmic ADC, which consumes $6 \text{ }\mu\text{A}$ from 2 V supply. This ADC topology is selected for its low power dissipation, adequate resolution for the target application, and low digital design complexity resulting in a small chip size in a $1.5 \text{ }\mu\text{m}$ CMOS process. A ratio-independent multiply-by-two scheme implemented by sampling the input voltage twice is used to

avoid capacitor mismatch limitations. The redundant signed digit (RSD) scheme employed by the ADC also improves its immunity to linearity errors caused by offset voltage and comparator accuracy.

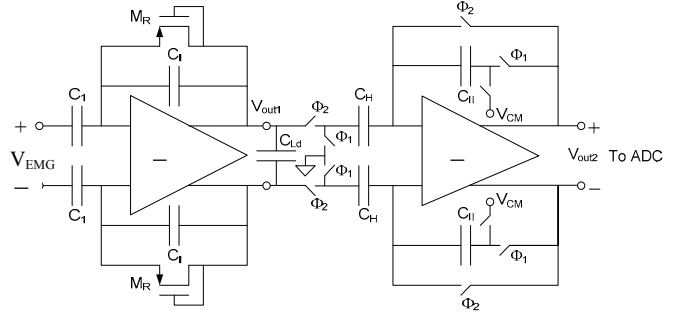


Figure 6. EMG interface electronics.

The digital output of the ADC is Manchester-coded and transmitted to an external transceiver by passive digital phase-shift keying (PSK) modulation scheme through the same wireless link used for RF powering. PSK modulation is achieved by digitally detuning the secondary (implanted) tank by means of a switching capacitor. This detuning action reflects a complex impedance back to the primary tank of the external transceiver, which is recovered by a phase detection circuit. Figure 7 presents the class-E RF power amplifier, inductive coupling elements, integrated rectification and regulation, PSK telemetry switch, and PSK demodulation circuitry. The PSK data is recovered by mixing the transmitter tank voltage with the 8 MHz clock. This process mixes the PSK data to baseband. The demodulated signal is low-pass filtered and then passed through a comparator to produce a digital output signal. The received RF power is converted into stable 2.1 V and 2.7 V supply lines to power the implant electronics. The 2.7 V supply is used to drive switched capacitor circuits.

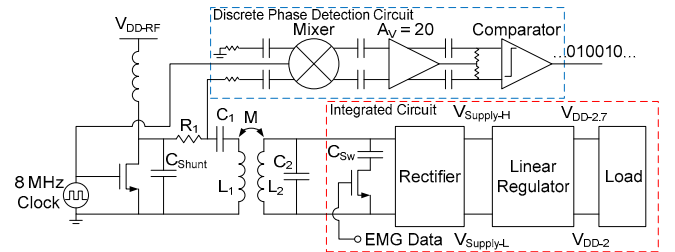


Figure 7. RF powering with PSK data telemetry architecture.

III. MEASUREMENT RESULTS

The custom integrated EMG sensing microsystem is fabricated in AMI $1.5 \text{ }\mu\text{m}$ 2-metal, 2-poly CMOS process. Figure 8 presents a micrograph of the integrated circuit, occupying $2.2 \text{ mm} \times 2.2 \text{ mm}$ area and consisting of an EMG front-end amplifier, $2.5\times$ switched-capacitor gain stage, algorithmic ADC, RF-DC power conversion electronics, PSK telemetry circuit, and digital control block, enclosed by

a 6 mm RF coil. The implantable electronics consume 83 μA from 2.1 V and 2.7 V supplies.

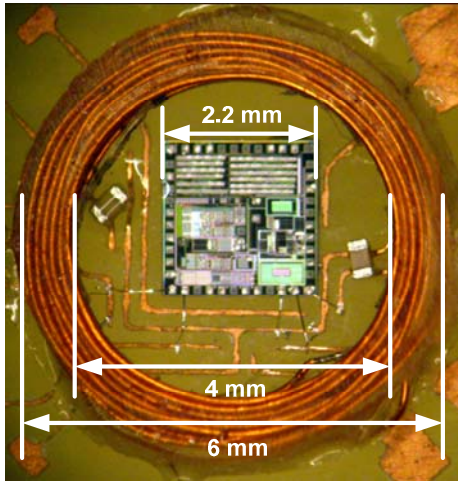


Figure 8. Prototype EMG sensing microsystem.

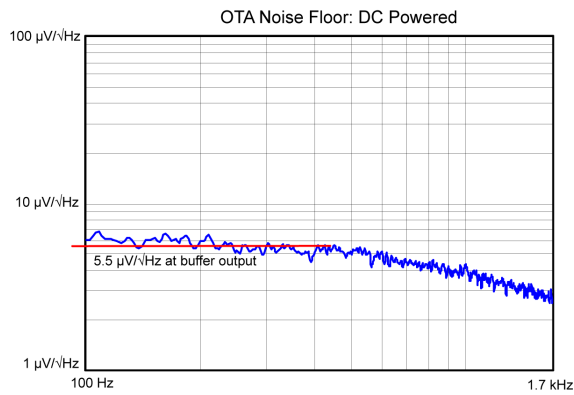


Figure 9. EMG amplifier thermal noise floor.

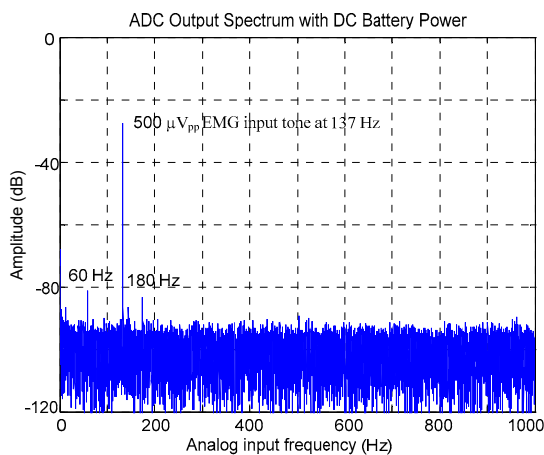


Figure 10. ADC digital output spectrum.

Figure 9 presents the output thermal noise floor of the EMG amplifier, from which the calculated input-referred noise is 78 $\text{nV}/\sqrt{\text{Hz}}$. The amplifier exhibits a low-pass corner frequency of approximately 920 Hz with a $1/f$ noise

corner frequency of 15 Hz, closely matching the design specifications. Figure 10 is the measured EMG amplifier output spectrum with a 500 $\mu\text{V}_{\text{p-p}}$ differential tone at 137 Hz applied to the EMG input. This tone represents a typical EMG signal level and frequency.

The overall microsystem is characterized for wireless powering and data telemetry. Two coils are aligned coaxially and separated by 1 cm. The implantable microsystem is powered up wirelessly and begins streaming digital test data back to the external transceiver. The Manchester-coded data can then be received and processed by a PC-based LabView program, as shown in Figure 11.

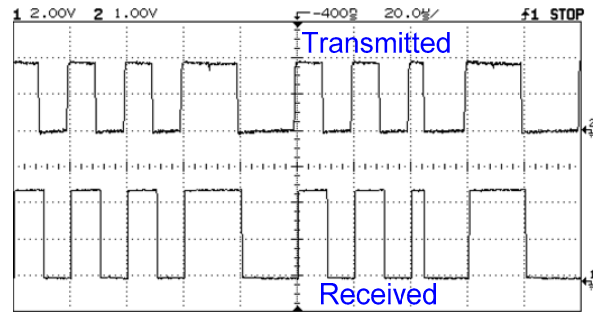


Figure 11. 50 kbps Manchester-coded PSK data telemetry.

IV. CONCLUSION

An implantable EMG sensing microsystem with wireless RF powering and PSK digital data telemetry for real-time monitoring of myoelectric signals is developed. The overall system consumes a low power of 83 μA from 2 V supply and demonstrated functionality adequate for a detailed *in vivo* EMG waveform suitable for intelligent myoelectric control of powered prosthetics.

ACKNOWLEDGMENT

The authors would like to thank the APT Center at the Cleveland VA for their financial support of this project.

REFERENCES

- [1] R. Z. M. Nikolic, D. B. Popovic, R. B. Stein, Z. Kenwell, "Instrumentation for ENG and EMG recordings in FES systems," *IEEE Trans. Biomedical Engineering*, v. 41, nr. 7, pp. 703-706, 1994.
- [2] N. Chaimanont, D. J. Young, "Remote RF powering systems for wireless MEMS strain sensors," *IEEE Sensors Journal*, v. 6, nr. 2, pp. 484-489, 2006.
- [3] M. Zimmerman, N. Chaimanont, and D. J. Young, "In vivo RF powering for advanced biological research," the 28th Annual International Conference of the IEEE Engineering in Medicine and Biology Society (EMBS '06), New York, N.Y., 2006, pp. 2506-2509.
- [4] N. Chaimanont, M. Suster, and D. J. Young, "Two-channel data telemetry with remote RF powering for high-performance wireless MEMS strain sensing applications," *Technical Digest, IEEE Sensors Conference*, Irvine, CA, October 2005, pp. 285-288.
- [5] R. R. Harrison, C. Charles, "A low-power low-noise CMOS amplifier for neural recording applications," *J. Solid State Circuits*, v. 38, nr. 6, pp. 958-965, 2004.
- [6] IEEE Standard for Safety Levels with Respect to Human Exposure to RF Electromagnetic Fields IEEE/ANSI c95.1.